

1 A Design for a Deep Underground Single-Phase
2 Liquid Argon Time Projection Chamber for
3 Neutrino Physics and Astrophysics

4 March 11, 2015

Contents

2	1 Detector Development Program	1
3	1.1 Introduction	1
4	1.2 Components of the Development Program	2
5	1.3 Scope and Status of Individual Components	2
6	1.3.1 Materials Test System	2
7	1.3.2 Photon Detection R&D	6
8	1.3.3 TPC Design	6
9	1.3.4 Electronics Development	7
10	CMOS Transistors: Lifetime Verification and Technology Evaluation	7
11	Readout Architectures, Multiplexing and Redundancy	9
12	1.3.5 35-ton Prototype Phase 1: Cryostat Development	9
13	1.3.6 35Ton Phase 1 Run	11
14	35T Instrumentation	13
15	35T Operations	15
16	Stability of Operation	20
17	Conclusions	23
18	1.3.7 35-ton Prototype Phase 2: TPC Installation and Operation . . .	23
19	TPC Design	23
20	Goals of the Phase 2 Test	23
21	Data Analysis and Future Applications	23
22	1.3.8 Physics Experiments with Associated Detector-Development Goals	23
23	ArgoNeuT - T962	25
24	MicroBooNE E-974	25
25	1.4 Summary	29

List of Figures

2	1.1	Liquid argon area at the Proton Assembly Building at Fermilab	4
3	1.2	Schematic of the Materials Test System (MTS) cryostat at Fermilab . .	5
4	1.3	Lifetime at different temperatures vs V_{DS}	8
5	1.4	Layout of 35-ton prototype at Fermilab's PC-4 facility	10
6	1.5	Membrane panel assembly and components	11
7	1.6	35T Cutaway Drawing.	12
8	1.7	35T Layout in PC4	14
9	1.8	Gas Ar Purge and Recirculation	16
10	1.9	35T Cooldown and Filling	17
11	1.10	35T Vapor Flow	19
12	1.11	35T Electron Lifetime	21
13	1.12	35T Temperature Stability	22
14	1.13	35T Vertical Temperature Profile	24
15	1.14	ArgoNeuT neutrino event with four photon conversions	26
16	1.15	Data from ArgoNeuT	26
17	1.16	ArgoNeuT: status of 3D reconstruction	27
18	1.17	ArgoNeuT: status of calorimetric reconstruction	28

¹ List of Tables

²	1.1	LBNE on-project development activities	3
³	1.2	LBNE off-project development activities	3
⁴	1.3	35T Details and Dimensions	13

1 **Todo list**

2	Move to Photon chapter?	6
3	Mark C asks: remove, or move to Electronics section?	7
4	Need explanation of phase 1 vs 2; unless covered above; need to check	11
5	11
6	15
7	18
8	18
9	20
10	23

Chapter 1

Detector Development Program

ch:randd

1.1 Introduction

This chapter describes the development program designed to ensure a successful and cost-effective construction and operation of the massive, dual-cryostat LArTPC detector for LBNE and to investigate possibilities for enhancing the performance of the detector. The feasibility of the LArTPC as a detector has been demonstrated most impressively by the current state of the ICARUS experiment currently taking data at Gran Sasso.

It is understood that for successful operation an LArTPC has stringent requirements on

- argon purity which must be of order 200 ppt O₂ equivalent or better
- long-term reliability of components located within the liquid argon; in particular, the TPC and field cage must be robust against wire-breakage and must support a cool-down of over 200 K
- the front-end electronics which must achieve a noise level ENC of 1000e or better

The design of the LBNE LArTPC has evolved significantly from earlier concepts based on standard, above-ground, upright cylindrical LNG storage tanks which envisioned single TPC sense and high-voltage planes spanning the full width of the tank – essentially a direct scaling of previous detectors. Problems with the actual construction of such massive planes and with the logistics of being able to construct the TPC only after the cryostat was complete are avoided in the present design. In our design, TPC ‘panels’ are fully assembled and tested – including the electronics –

independently of the cryostat construction. This modular approach is a key feature of the design. It has the benefit not only of improving the logistics of detector construction, but also the individual components can be of manageable size. It should also be noted that the cryostat itself is formed of modular panels designed for quick and convenient assembly.

1.2 Components of the Development Program

Programs of ongoing and planned development to allow the construction of massive LArTPCs in the U.S. have been developed and described in the *Integrated Plan for LArTPC Neutrino Detectors in the US* [?]. To advance the technology to the detectors proposed for LBNE, the U.S. program has three aspects:

- a demonstration that the U.S program can reproduce the essential elements of the existing technology of the ICARUS program
- a program of development on individual elements to improve the technology and/or make it more cost-effective
- a program of development on how to apply the technology to a detector module

A summary of the items in the program is given in the following tables. Table 1.1 lists the activities that are part of the LBNE Project (“on-project”) described in this chapter, a short description of the information needed and the LBNE milestone corresponding to when the information is required. Table 1.2 lists off-project activities, the aspect of these activities that is applicable to LAr-FD and the LBNE milestone at which the information is required. These aspects will be described in more detail in the following sections. As will be explained below, these are not R&D activities, but rather elements of the preliminary engineering design process.

1.3 Scope and Status of Individual Components

1.3.1 Materials Test System

An area for LAr detector development, shown in Figure 1.1, has been established in the Proton Assembly Building at Fermilab. The Materials Test System (MTS) has been developed to determine the effect on electron-drift lifetime of materials and components that are candidates for inclusion in LAr-FD. The system essentially consists of a source of clean argon (< 30 ppt O_2 equivalent), a cryostat, a sample

Table 1.1: LBNE on-project development activities

Activity	LAr-FD Information	Need by
In-liquid Electronics	Low noise readout, long lifetime	CERN prototype construction
TPC Construction	Mechanical design	CERN prototype construction
35-ton Prototype	Cryostat construction	CERN prototype cryostat procurement
CERN prototype	detector integration	TPC construction

Table 1.2: LBNE off-project development activities

Activity	LAr-FD Applicability	Status	Need by
Yale TPC	None	Completed	NA
Materials Test System	Define requirements	Completed	NA
	Materials testing	Operating	As Req'd
Electronics Test Stand	Electronics testing	Operating	As Req'd
LAPD	Purity w/o evac.	Operating	LBNE CD-2
	Convective flow	Operating	LBNE CD-2
Scintillator Development	Photon Det. Definition	Completed	CERN prototype Construction
	Industrialization	Not started	LBNE CD-3
ArgoNeuT	Analysis tools	On-going	LBNE CD-2
MicroBooNE	Electronics tests	Construction	LBNE CD-3
	DAQ algorithms	In development	LBNE CD-3
	Analysis tools	In development	LBNE CD-2
	Lessons learned	Not started	LBNE CD-3

1 chamber that can be purged or evacuated, a mechanism for transferring a sample
 2 from the sample chamber into the cryostat, a mechanism for setting the sample
 3 height in the cryostat so that it can be placed either in the liquid or in the gas ullage
 4 above the liquid, a temperature probe to measure the temperature of the sample,
 5 and an electron-lifetime monitor. The system is fully automated and the lifetime
 6 data are stored in a single database along with the state of the cryogenic system.



Figure 1.1: Liquid argon area at the Proton Assembly Building at Fermilab

PAB

7 A noteworthy feature is the novel bubble-pump filter inside the cryostat. In case
 8 of argon contamination, this can filter the cryostat volume in a few hours, allowing
 9 us to continue studies without having to refill. A schematic of the MTS is shown in
 10 Figure 1.2.

11 The major conclusions of the studies to-date are summarized here. No material
 12 has been found that affects the electron-drift lifetime when the material is immersed
 13 in liquid argon – this includes, for example, the common G-10 substitute, FR-4. On
 14 the other hand, materials in the ullage can contaminate the liquid; this contamination
 15 is dominated by the water outgassed by the materials and as a result is strongly
 16 temperature-dependent. Any convection currents that transport water-laden argon

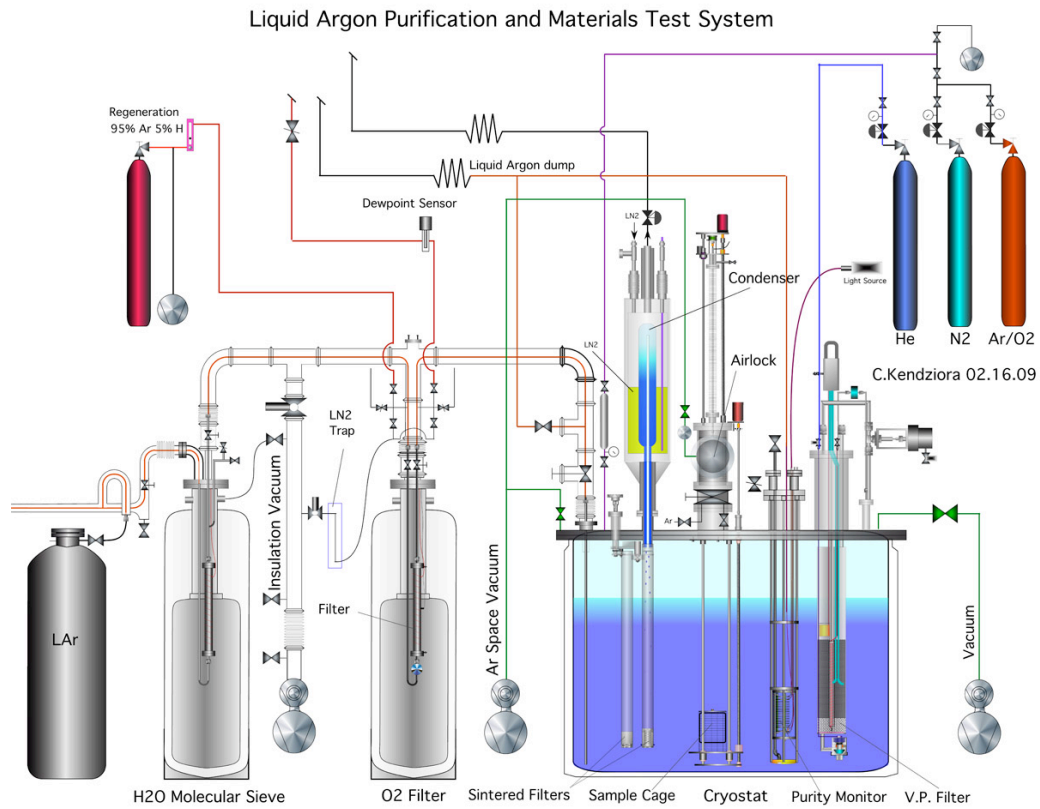


Figure 1.2: Schematic of the Materials Test System (MTS) cryostat at Fermilab

MTS_Schem

into the LAr and any cold surfaces on which water-laden argon can condense will fall into the LAr and reduce the electron lifetime. Conversely, a steady flow of gaseous argon of a few ft/hr away from the LAr prevents any material in the gas volume from contaminating the LAr.

These results are taken into account in the design of both MicroBooNE and LAr-FD. For LBNE they have been cast as detector requirements. The MTS will continue to be used by MicroBooNE and LBNE to test detector materials such as cables that will reside in the ullage.

1.3.2 Photon Detection R&D

Move to Photon chapter?

The R&D program for Photon Detection is based on a promising, new, cost-effective scheme for light collection in LArTPCs as described in a NIM article by Bugel et al [?]. The design is based upon lightguides fabricated from extruded or cast acrylic and coated with a wavelength-shifter doped skin. Multiple acrylic bars are bent to guide light adiabatically to a single cryogenic PMT. Prototypes of the basic detector elements have been shown to perform well. These lightguides have a thinner profile than the usual TPB-coated PMT-based system, occupying less space in an LAr vessel and resulting in more fiducial volume. Another advantage of this system is that the bars are inexpensive to produce. The most convenient place for the paddles is between the wire planes that wrap around the APAs.

Lightguide R&D has advanced rapidly since the initial publication resulting in $\sim 3 \times$ higher light yields. The R&D is now sufficiently advanced to provide a technical basis for the LAr-FD reference design. On-going design efforts at MIT, Indiana University, and Fermilab are directed toward industrial-scale production and the evaluation of lower-cost fluors that are effective in converting VUV photons. These efforts also include investigating PMTs with increased quantum efficiency as well as other efficient light-collection technologies, such as Geiger-mode avalanche photodiodes (commonly known as Silicon Photomultipliers, or SiPMs).

1.3.3 TPC Design

The design for LBNE has adopted the basic ICARUS multi-plane, single-phase TPC concept and has incorporated new features suitable for a very large detector. The main emphasis of the development program is to develop a TPC design that is highly modular, low-cost, robust and easily installed inside a finished cryostat.

1 A significant effort has been focused on minimizing the dead space between de-
 2 tector modules to improve the fiducial versus total LAr-volume ratio. The APA
 3 reference design accomplishes this goal but requires making ~ 2 million high-quality
 4 wire terminations. The wire-termination scheme used by ICARUS has proven to be
 5 very reliable but it is too labor-intensive to fabricate for a million-channel detector
 6 system. We have adopted the wire-solder + wire-epoxy termination scheme that has
 7 been used for decades on drift chambers and proportional wire chambers to mount
 8 Cu-Be wires. The termination scheme was used to terminate 2.5 million anode wires
 9 in the CMS end-cap muon system. Cu-Be wires have excellent mechanical properties
 10 and the advantage of low resistance compared to stainless steel. A study is currently
 11 underway within the LAr-FD subproject to identify the optimum wire-bonding pa-
 12 rameters. The focus is currently on finding a commercial epoxy that optimizes the
 13 qualities of bond strength, cure time and low-temperature operation.

14 1.3.4 Electronics Development

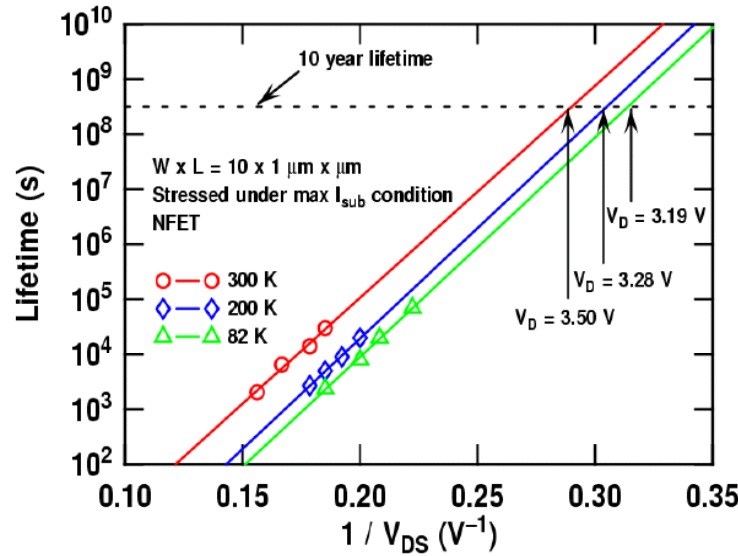
15 Mark C asks: remove, or move to Electronics section?

16 The work to-date on cold electronics has established that no show-stoppers ex-
 17 ist. The remaining activities outlined here concern performance optimization of the
 18 CMOS ASICs, the evaluation of several widely available CMOS technologies, and the
 19 development of readout architectures appropriate and timely for various scenarios of
 20 very large detectors.

21 CMOS Transistors: Lifetime Verification and Technology Evaluation

22 The results of the design of the CMOS electronics for operation at LAr temperature
 23 (89 K), performed so far by the MicroBooNE and LBNE collaborations, as well
 24 as by a large collaboration led by Georgia Inst. of Technology, are summarized in
 25 Section ??.

26 Briefly, the fundamentals are: charge-carrier mobility in silicon increases at 89 K,
 27 thermal fluctuations decrease with kT/e , resulting in a higher gain (trans conduc-
 28 tance/current ratio = g_m/i), higher speed and lower noise. For a given drain-current
 29 density the same degree of impact ionization (measured by the transistor substrate
 30 current) occurs at a somewhat lower drain-source voltage at 89 K than at 300 K.
 31 The charge trapped in the gate oxide and its interface with the channel causes degra-
 32 dation in the transconductance (gain) of the transistor and a threshold shift. The
 33 former is of major consequence as it limits the effective lifetime of the device (defined
 34 in industry and the literature as 10% degradation in transconductance). Thus an

Figure 1.3: Lifetime at different temperatures vs V_{DS}

DSV

1 MOS transistor has equal lifetime due to impact ionization at 89 K and at 300 K at
 2 different drain-source voltages. This is illustrated in Figure 1.3.

3 This feature offers a tool for accelerated-lifetime testing by stressing the transis-
 4 tor with both increased current and increased voltage, and monitoring the substrate
 5 current and the change in g_m due to impact ionization. In these conditions, the
 6 lifetime can be reduced arbitrarily by many orders of magnitude, and the limiting
 7 operating conditions for a lifetime in excess of ~ 20 years can be determined. With
 8 this foundation, more conservative design rules (lower current densities and voltages)
 9 can be derived and applied in the ASIC design, as has been done for the ASIC de-
 10 scribed in Section ???. The goal of this part of the program is to verify by accelerated
 11 testing the expected lifetimes for the several widely available CMOS technologies
 12 under consideration (TSMC, IBM, AMS). It should be noted that this is a standard
 13 test method used by the semiconductor industry. These methods are used to qualify
 14 electronics for deep space NASA missions as well as commercial PCs.

1 Readout Architectures, Multiplexing and Redundancy

A high degree of multiplexing after digitization of signals is essential for a TPC with 0.5 million wires in order to reduce the cable plant and the attendant outgassing. Just how high a multiplexing factor should be chosen is a matter of study, considering the risk of losing one output data link. A part of the program will include system designs with redundant links and redundant final multiplexing stages to minimize the risk of losing the data from a significant fraction of the TPC (note that even with a multiplexing factor of 1/1024 and no redundancy, one failed link would result in a loss of 0.2%).

1.3.5 35-ton Prototype Phase 1: Cryostat Development

The next step in the cryostat-prototype program is intended to address project-related issues: (1) to gain detailed construction experience, (2) to develop the procurement and contracting model for LAr-FD and (3) to incorporate the design and approval mechanism in the Fermilab ES&H manual. (Membrane cryostats are designed in accordance with European and Japanese standards.) At present, we are in the process of procuring the cryostat components for a 35-ton membrane cryostat from IHI.

The LBNE project has contracted with the Japanese company IHI to build a small prototype membrane cryostat at Fermilab. This approximately 35-ton unit is to be built and made operational in 2012 at Fermilab's PC-4 facility where LAPD is located. It is intended to demonstrate high-purity operation in this type of cryostat and the suitability of the planned LAr-FD construction techniques and materials. The testing programs for LAPD and the small prototype will be similar. LBNE's 35-ton membrane cryostat will use a large portion of the cryogenic-process equipment installed for LAPD.

The prototype membrane cryostat's total size, including insulation and concrete support, is approximately 4.1 m \times 4.1 m \times 5.4 m, and will hold approximately 826 tons of LAr. The insulation thickness will be 0.4 m rather than the 1.0 m chosen for our reference design. The techniques of membrane-cryostat construction will be demonstrated to be a fit for high-purity TPC service. Welding of corrugated panels, removal of leak-checking dye penetrant or ammonia-activated leak-detecting paints, and post-construction-cleaning methods will be tested for suitability of service. Residual contamination measurements at different elevations during the initial GAr purge process will be compared to computational predictions and will validate the purge-process modeling of a large rectangular vessel. The prototype membrane cryostat will be filled with LAr. Purity levels of the liquid with time and electron-drift

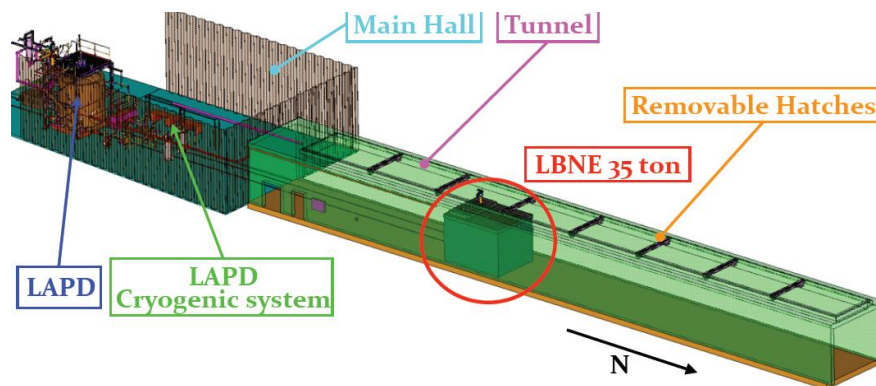


Figure 1.4: Layout of 35-ton prototype at Fermilab's PC-4 facility

fig:v5ch2-35ton

1 times will be measured using purity monitors installed in the liquid bath. Heat-load
 2 measurements will be made and compared to calculations. Eventually, connectors
 3 and feedthroughs, ports and other features that are planned for the reference design
 4 will be incorporated into the prototype. Materials and cold-electronics testing can
 5 be done along with electron-drift-time measurements.

6 In principle, a thin-walled membrane cryostat is as suitable as a thick-walled
 7 cryostat for use with high purity LAr. Both would be constructed with 304 stainless
 8 steel with a polished surface finish. Both would use passive insulation. The total
 9 length of interior welds required for construction would be similar in both cases. The
 10 leak checking procedure would be the same in both cases.

11 The significant difference between membrane cryostats and thick-walled cryostats
 12 is the depth of the welds used to construct the vessel. The majority of membrane-
 13 cryostat welds are completed in one or two passes with automatic welding machines.
 14 A second difference, and a major advantage, is that the membrane cryostat is a
 15 standard industrial design that has been in use for over 40 years. A thick-walled
 16 cryostat vessel would be custom designed and would require significant engineering
 17 and testing. A third difference, and another major advantage, is the ability to purge
 18 the membrane cryostat insulation space with argon gas so that a leak cannot affect
 19 the purity if it escapes detection and repair.



Figure 1.5: Membrane panel assembly and components

3panel

A 3-m \times 3-m wall panel shown in Figure 1.5 was constructed at Fermilab using materials and technical guidance from GTT. The labor hours used in construction are consistent with the vendor estimates. The wall panel was leak tested (none were found) and vacuum tests were performed on the insulation system. We found that the insulation system is designed to allow vacuum pumping of the main cryostat volume to a hard vacuum. This result demonstrates that vacuum pumping of a membrane cryostat is feasible, if it is found to be required. No modifications to the vendor-supplied components are required to accomplish this.

1.3.6 35Ton Phase 1 Run

The 35-ton Prototype Cryostat (35T) is a small demonstration project to show the suitability of the membrane technology for LAr detectors. In particular that it can achieve and hold the needed purity levels and provide a stable environment for the TPC. A cutaway drawing of the 35T is shown in Figure 1.6.

Need explanation of phase 1 vs 2; unless covered above; need to check

The 35T was constructed in 2012 in a decommissioned beam line (Proton Center) at Fermilab. This location is adjacent to another LAr cryostat, the Liquid Argon Purity Demonstrator (LAPD) [1].

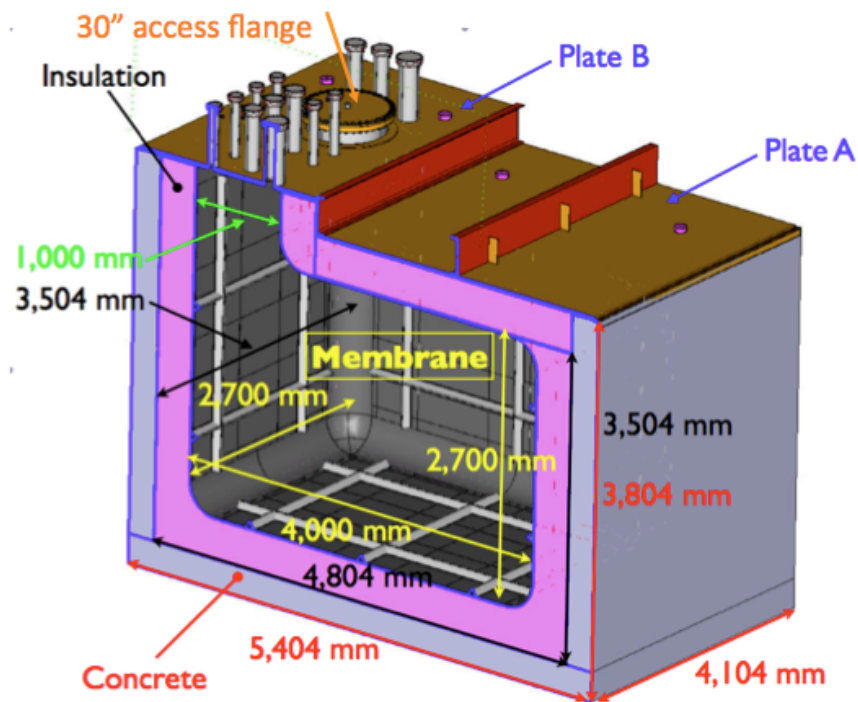


Figure 1.6: Cutaway drawing of the 35 Ton Cryostat showing construction details with exterior and interior dimensions.

fig:cutaway

This enabled the 35T to reuse the existing purification and instrumentation infrastructure of LAPD (see Figure 1.7). The proximity and size (30 tons) of LAPD also offers the possibility using LAPD as a partial storage vessel for LAr if the 35T would need to be emptied. The 35T employs a submersible LAr pump to pump the LAr from the cryostat to the filters. Two pumps were installed for redundancy, but only one is used at a time.

Table 1.3 gives the details of the construction materials and the dimensions for the 35T. More information can be found in [2].

Table 1.3: 35T Details and Dimensions

Parameter	Value
Cryostat Volume	29.16 m ³
Liquid Argon total mass	38.6 metric tons
Inner dimensions	4.0 m (L) x 2.7 m (W) x 2.7 m (H)
Membrane	2.0 mm thick corrugated 304 SS
Insulation	0.4 m polyurethane foam
Secondary barrier system	0.1 mm thick fiberglass
Vapor barrier Normal	1.2 mm thick carbon steel
Steel reinforced concrete	0.3 m thick layer

35T Instrumentation

The 35T includes a full complement of standard commercial transducers and sensors that are used to monitor and control the cryogenic environment. They include temperature sensors, pressure transducers (absolute and gauge), flow meters, and level sensors. These devices are typically readout directly into the Control System and data logged.

A number of commercial gas analyzers are available that can measure trace impurity levels (O₂, H₂O, and N₂) in the argon. Some have sensitivities at the 100 ppt level. A gas distribution switchyard feeding the gas analyzers allows the sampling points in the 35T to be reconfigured.

There were also two purpose-built pieces of instrumentation for the monitoring of the high-purity environment needed for a LAr detector. They are the purity monitors (PrMs) and the RTD Spooler. The PrMs are used to measure electron lifetimes in the LAr, and the RTD Spooler is used to make precision measurements

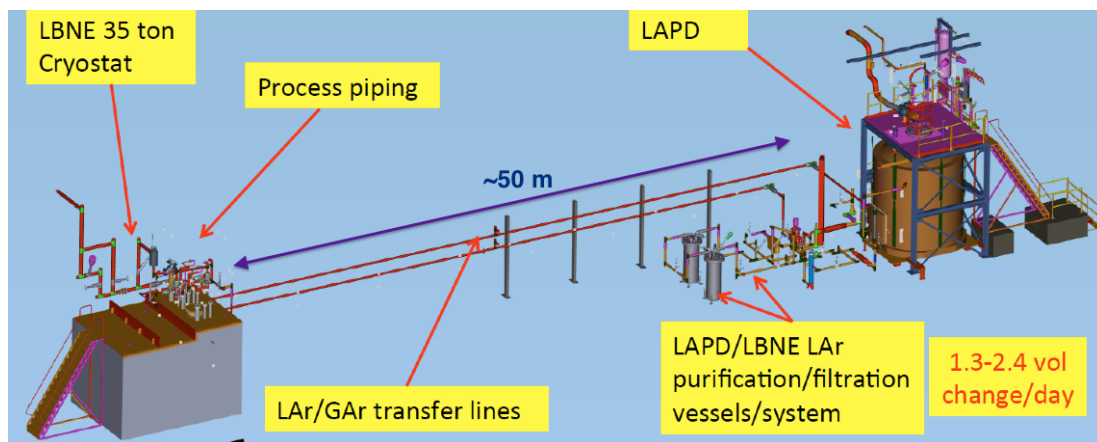


Figure 1.7: Drawing of arrangement of the 35T and LAPD in Proton Center beam line.

Design for a Deep Underground Single-Phase LArTPC

fig:35TLayout

of the temperature profile of the cryostat as a function of depth. These instruments were originally constructed for the LAPD run and are described in depth in [1]

35T Operations

In order to purify LAr, it is necessary to do three things: 1) remove the air from the cryostat, leaving only Ar gas, 2) clean the liquid Ar as it comes from the supplier, and 3) remove any impurities that are generated by materials outgassing within the cryostat. LAPD has demonstrated that it is not necessary to evacuate a cryostat in order achieve LAr purity levels sufficient for LBNE. This is of paramount importance since the costs of multi-kiloton cryostats that could withstand evacuation is prohibitive. The 35T followed the procedure LAPD [1] established to obtain and maintain pure LAr.

A. Gas Phase

Figure 1.8 graphically shows step 1, removing the ambient air, of the purification process. These measurements are made by a variety of gas monitors that are sampling the gas in the cryostat.

The initial state of the 35T was that “dry” air had been purging the cryostat for approximately three weeks. The initial start values for oxygen, water, and nitrogen reflect this state. The air in the cryostat is removed by the Piston Purge. Argon gas is flooded into the bottom of the cryostat. As argon is heavier than air, the argon layer rises analogous to a mechanical piston, pushing the air up and out of the cryostat. This gas is vented to the outside atmosphere. The venting stage continues for 32 hours, approximately the equivalent of 12 volume changes.

At this point the exiting gas is re-routed to circulate through the filtration system that removes O_2 and H_2O . N_2 is not materially removed by the filters. Any leaks to the outside atmosphere can be detected during this step. As shown in Figure 1.8, a leak was found and mitigated (the “Debugging” gap in the plot). Once leaks have been eliminated the recirculation continues until the O_2 level drops into the sub-ppm level. As can be seen in the plot, the H_2O level plateaus at a much higher level than O_2 . This is due to the outgassing of materials inside the 35T, including the cryostat walls, which are at room temperature during the recirculation step.

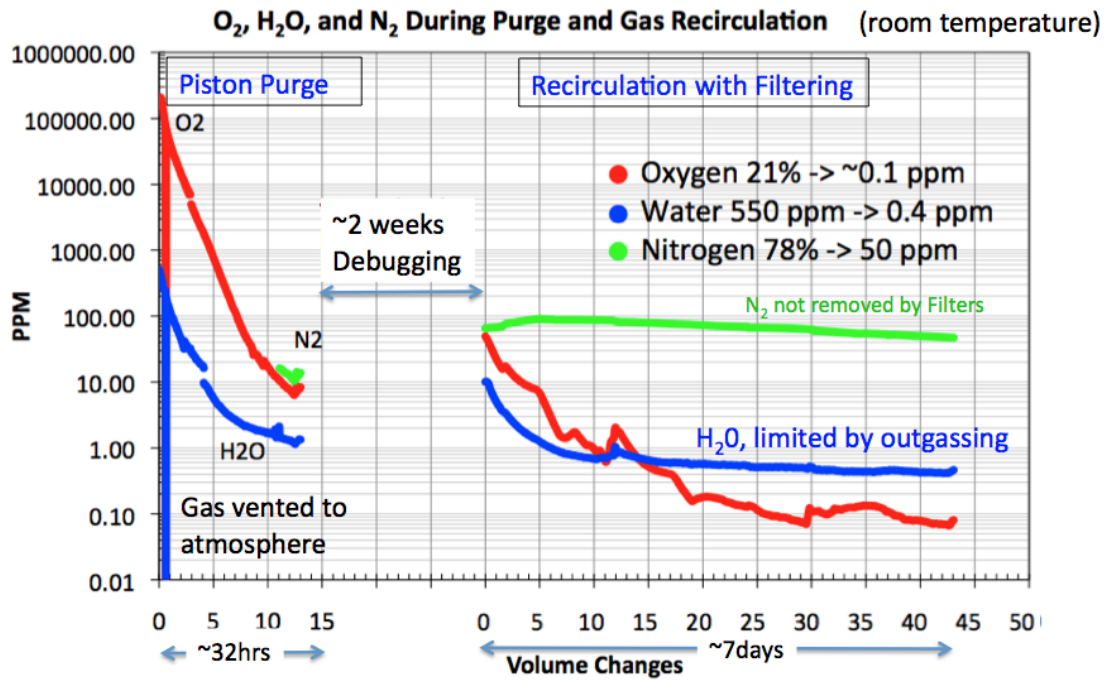


Figure 1.8: Gas phase of removing impurities in the 35T. These quantities are being measured by various gas analyzers. The first stage of the purification is a process called the “Piston Purge”. The second stage is “Recirculation with Filtering”. The gap between the two steps was due to troubleshooting a leak.

fig:35TPurge

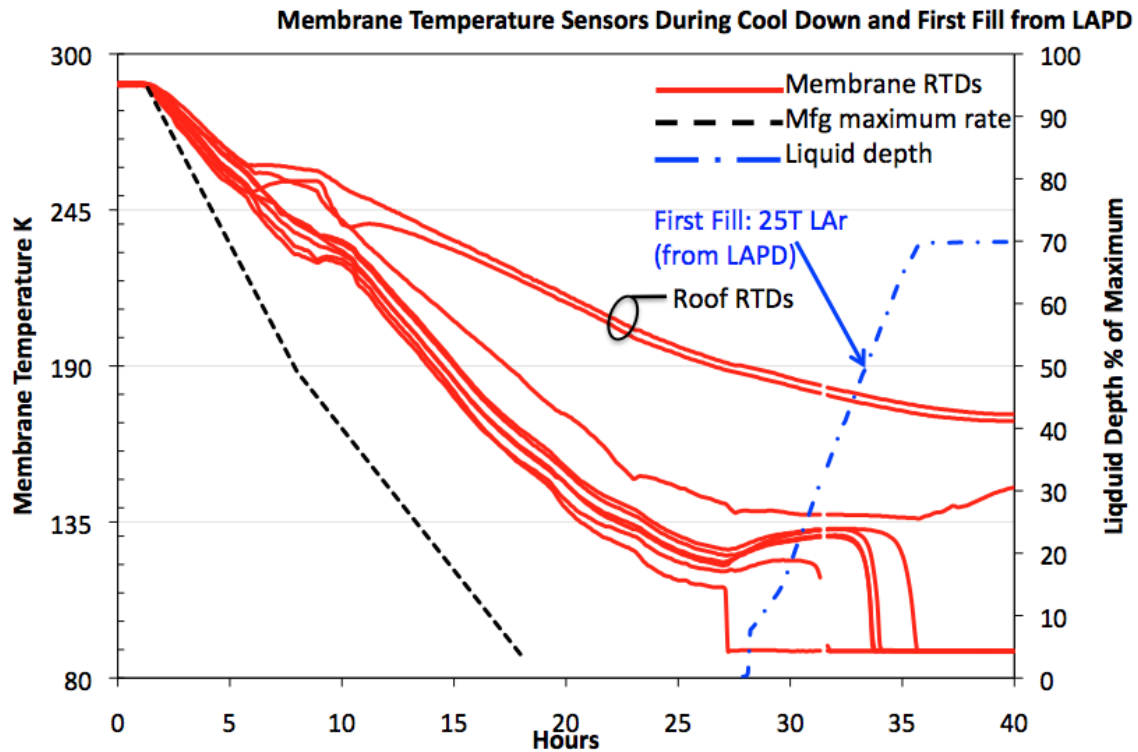



Figure 1.9: Cooldown and filling the 35T. The measurements (red trace) are made from RTDs afixed to the cryostat walls. The black dashed curve is the manufacturer's maximum allowed cooldown rate. The filling (blue trace) was from the transfer of LAr from LAPD, This quantity of LAr is less than the capacity of the 35T. The RTD traces drop to the LAr temperature when the level of the LAr covers reaches their mounting height.

fig:35TCooldown

1 B. Cool down and LAr filling


2 We have adopted a gas/liquid spray method to cool down the cryostat. This generates
 3 a turbulent mixing of cold gas in the cryostat and cools the entire surface. The cool
 4 down rate was limited to be less than the maximum rate specified by the membrane
 5 cryostat manufacturer. The cool down, as well as the initial filling is shown in
 6 Figure 1.9 . The temperature measurements (red traces) in this plot were made by
 7 RTDs that are glued to the membrane walls of the cryostat. The black dashed trace
 8 is the manufacturer specification for the cool down rate.

9 Once the cool down was finished, the LAr transfer into the cryostat began. In
 10 the case of the 35T phase 1 run, the LAr came from LAPD, where it had been used
 11 by that system in its own recently completed second run [1]

12 
 13 .
 14 LAPD contained about 30 tons of LAr, of which only 25 tons could be transferred
 15 to the 35T (~70% of the total possible 35T LAr volume). It was decided that we
 16 would begin the initial commissioning of the Phase 1 run with this level since several
 17 components of the 35 Ton could be commissioned with the partial LAr fill. After
 18 running with this partial fill for approximately eighteen days, additional LAr was
 19 added to bring the capacity to 100%.

20 C. LAr Purification

21 The Fermilab Material Test Stand (MTS) [4]

22 
 23 has shown that contaminants released inside LAr filled cryostats are from mate-
 24 rials outgassing in the warm ullage regions above the LAr surface. Typical detector
 25 materials located in LAr have negligible impact of LAr purity levels.

26 Figure 1.10 depicts how impurities generated by outgassing materials in the rel-
 27 atively warm ullage under Plate B are swept up by the normal Ar boil-off in the
 28 35T. This impure vapor is condensed in the LN2-cooled LAr condensor. The im-
 29 pure condensate is returned to the 35T just inside the intake manifold of the interior
 30 submersible LAr pump. From there it is pumped to the filtration system where the
 31 impurities are removed.

32 Of interest, the electron lifetime of the LAr exiting the filters, as measured by
 33 the inline PrM was always > 30 ms (purity ~ 10 ppt O₂ equivalent). This indicates
 34 that the filters are very efficient at removing all trace amounts of O₂ and H₂O. This
 35 was true for the entire 35T phase 1 run, including the filling periods.

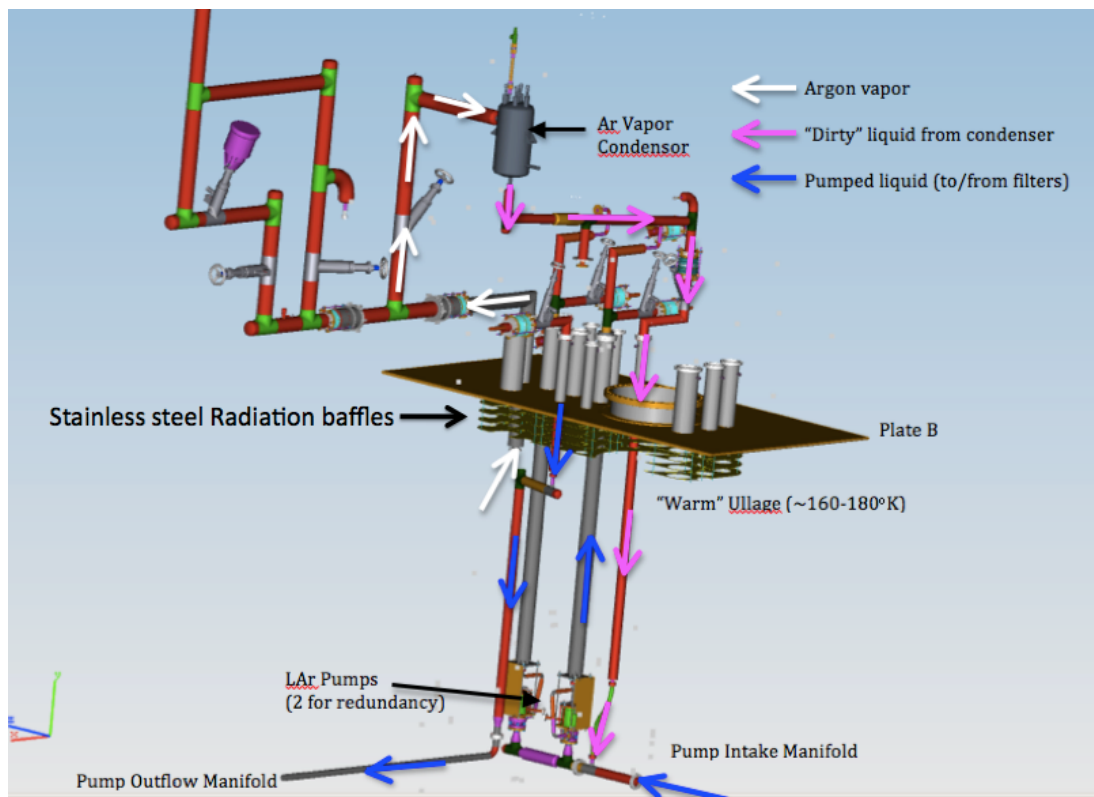


Figure 1.10: Drawing of Boiloff/Outgassing Vapor Flow (white arrows) from the Cryostat, with condensate return (violet arrows) from the condenser into the Pump Intake Manifold. LAr flow into the pump, and return from the Purification filters are shown by blue arrows. Also shown is the location of the Stainless Steel Radiation baffles beneath Plate B. This location just beneath Plate B is the warmest location and presumably the principal source of outgassing within the cryostat.

Figure 1.11 shows the electron lifetime from the start of the LAr Pump operation until the Phase 1 run ended. In general the electron lifetime improved as a function of pump on-time, but there were several incidents that spoiled the lifetime. These will be discussed in the next section.

Stability of Operation

The goals of the 35T Phase 1 run include not only achieving the required purity/lifetime levels, but to also hold those levels and provide a stable operation of the cryostat. The 35T Phase 1 run was a relatively short 2 months of LAr running. We achieved electron lifetimes in the 2-3 ms range as can be seen in Figure 1.11.

However the electron lifetimes were severely impacted whenever we would switch from one LAr pump to another. The drops in purity coincided with the turn on of the previously-inactive pump (see annotations in Figure 1.11). We believe the issue was with the procedure we used to start the pumps and plan to modify it for future operations in the 35T Phase 2 run.

A second stability question is keeping the temperature stable in the cryostat. Currently the 35T controls system regulates the gauge pressure of the cryostat, keeping the internal pressure to 6.69(02) kPa above ambient atmospheric pressure. However this leaves the thermodynamics of the LAr sensitive to normal atmospheric pressure changes.

Figure 1.12 is a plot over a nine day period of the Cryostat absolute pressure (blue trace), bulk LAr temperature (white dashed trace) and the normalized drift time of three PrMs, one short and long inside the cryostat, and the long inline PrM exterior to the cryostat. The temperature is taken from the RTD Spooler measurements by requiring that the RTDs be at least 15 cm below the LAr surface. The temperature curve lags the pressure changes ($\Delta P \sim 3.5$ kPa over this period), due to the thermal inertial of the LAr. However the normalized drift time (= drift time/(average drift time for this period) is directly correlated to the LAr temperature. The LAr temperature excursion range was $\Delta T \sim 0.3$ K. Fitting the normalized drift velocity (inverse of normalized drift time) gives the result

$$\Delta_{\text{driftspeed}/\text{driftspeed}} = -0.022/001 \text{ K}$$

The electron drift velocities for these three PrMs varied from (0.3 to 0.4) mm/ μ s depending on the individual PrM's drift field.

The RTD Spooler was intended to give us a precision measurement of the vertical temperature profile. This measurement is a means of testing the Computational Fluid Dynamics Simulations [5]

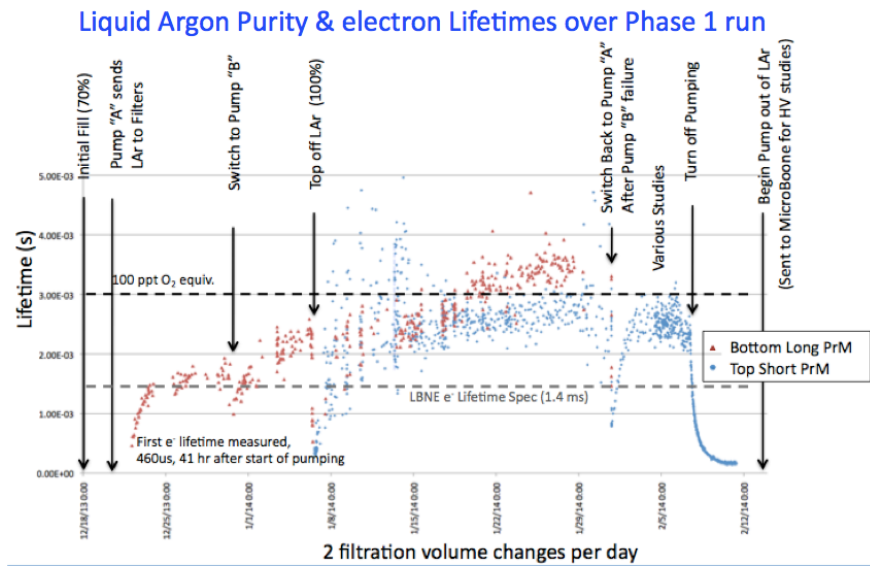


Figure 1.11: LAr electron lifetimes as measured by Cryostat Purity Monitors. Significant events are annotated on the plot. Major divisions on horizontal axis are one week periods. Equivalent purity levels are shown as dashed horizontal lines.

fig:35TElectro

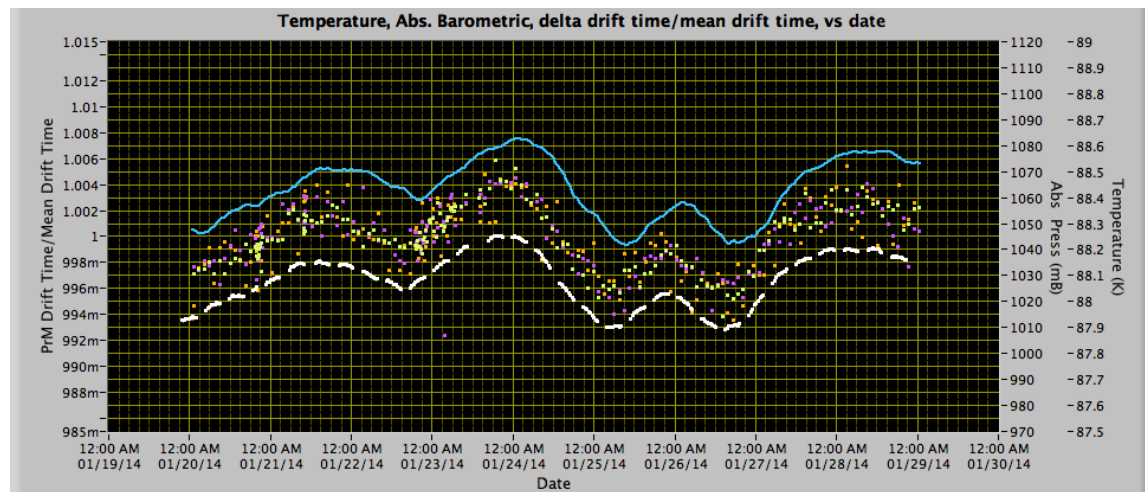


Figure 1.12: Interior Cryostat Absolute Pressure (blue trace), bulk LAr temperature (white dashed trace), and PrM drift times (dots) over a nine-day period. Major divisions on horizontal axis are one day intervals. The PrM drift times are from three PrMs, two in the cryostat, and the third from the inline PrM. The lag between the temperature and pressure is due to the 35T thermal inertia.

fig:35TTempSta

that are being made on the fluid motion in the cryostat. Experimentally measuring the actual motion does not appear to be feasible at this time. The CFD calculations are being used to understand whether there might be dead areas in the cryostat where impurities might collect. Figure 1.13 shows the result of one RTD scan. This scan was taken from a period where the barometric pressure was relatively constant so that the temperature would remain constant during the scan. Since a scan takes up to 6 hours in one direction (up or down) and as can be seen in Figure 1.12, pressure changes can impact the bulk temperature of the LAr. These profiles seen in Figure 1.13 are in nominal agreement with the current CFD calculations [5].

Conclusions

The 35T Phase 1 run has shown that the membrane cryostat technology has no innate difficulties with achieving the stated goals of the LBNE Conceptual Design Far Detector. Some of the 35T issues (e.g. loss of purity when pumps are switched) are most likely unique to the 35T. It also seems likely that in a future design, the pumps will be externally located, to avoid coupling acoustical vibrations into the Far Detector cryostat and to facilitate maintenance and repair.

1.3.7 35-ton Prototype Phase 2: TPC Installation and Operation

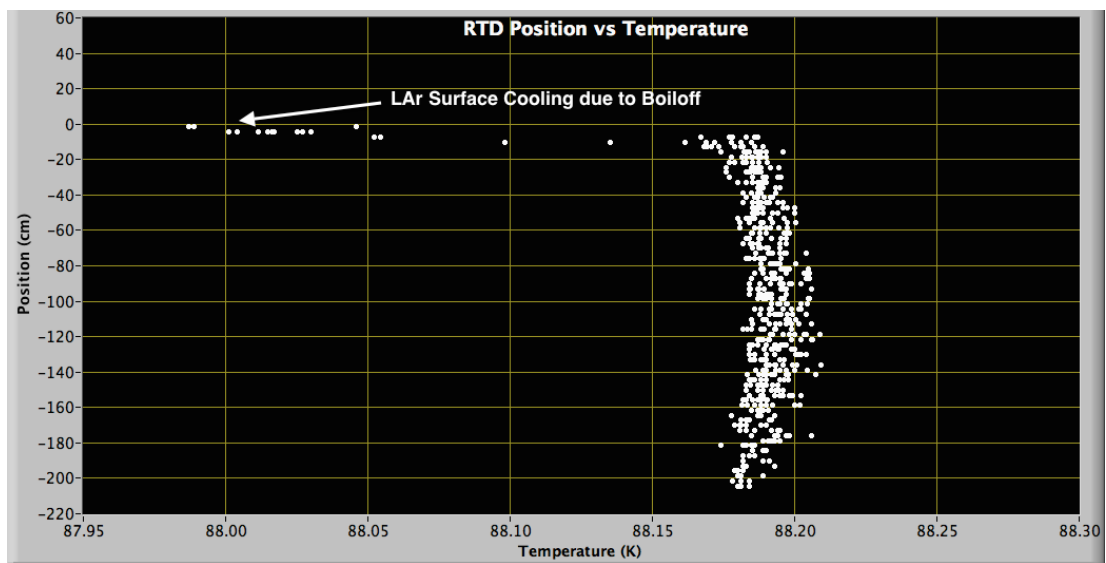
TPC Design

Goals of the Phase 2 Test

Data Analysis and Future Applications

1.3.8 Physics Experiments with Associated Detector-Development Goals

Two projects, ArgoNeuT and MicroBooNE, which are physics experiments in their own right, are also contributing to the development of the LBNE experiment. Their most important role is in providing data and motivation for the development of event reconstruction and identification software.



Design for a Deep Underground Single-Phase LArTPC

ArgoNeuT - T962

The Argon Neutrino Test (ArgoNeuT) is a 175-liter LArTPC which completed a run in the NuMI neutrino beam. The $0.5\text{ m} \times 0.5\text{ m} \times 1\text{ m}$ LArTPC was positioned directly upstream of the MINOS near detector, which served as a muon catcher for neutrino interactions occurring in ArgoNeuT.

ArgoNeuT began collecting data using the NuMI anti-muon neutrino beam in October 2009 and ran until March 1, 2010. ArgoNeuT's $\sim 10\text{k}$ events motivate the development of analysis tools, and are the basis for the first measurements of neutrino cross sections on argon. An event with two π^0 decays is shown in Figure ??.

ArgoNeuT was also the first LArTPC to be exposed to a low-energy neutrino beam and only the second worldwide to observe beam-neutrino interactions. The ArgoNeuT collaboration is currently preparing (1) a NIM paper that documents the detector performance using NuMI beam muons and (2) the first physics paper on muon-neutrino charged-current differential cross sections on argon. See Figures 1.16 and 1.17.

A deconvolution scheme using an FFT has been applied to the ArgoNeuT data. This procedure eliminates a problem with the ArgoNeuT electronics (which were D-Zero spares and could not be modified for ArgoNeuT). Another more significant benefit of deconvolution is that bi-polar induction-plane signals can be transformed into uni-polar collection-plane signals. An example of this is shown in Figure ?. A selection of figures from the draft NIM paper are reproduced below.

The applicability of ArgoNeuT is that it provides a set of data in the same range of energy as the LBNE neutrino beam, enabling the development of analysis algorithms that can be utilized for LAr-FD physics analysis with little or no modification.

MicroBooNE E-974

The MicroBooNE experiment is an 89-ton active mass LArTPC, (170-ton argon mass) in the commissioning phase. It has both a physics program and LArTPC development goals.

MicroBooNE received stage 1 approval from the Fermilab director in 2008, partial funding through an NSF MRI in 2008 and an NSF proposal in 2009. MicroBooNE received DOE CD-0 Mission Need in 2009, CD-1 review in 2010, CD-2/3a review in 2011, CD-3b review in 2012 and CD-4 review in December 2014. The construction of MicroBooNE experiment has been completed successfully, and detector commissioning is ongoing. It plans to start running in mid 2015.

As well as pursuing its own physics program, MicroBooNE will collect a large sample ($\sim 100\text{k}$) of low-energy neutrino events that will serve as a library for the

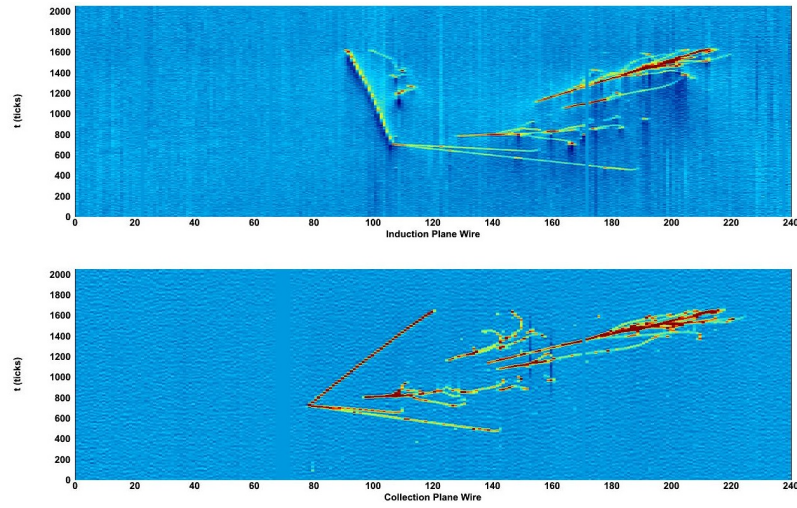


Figure 1.14: A neutrino event with four photon conversions in the ArgoNeuT detector. The top (bottom) panel shows data from the induction (collection) plane after deconvolution.

2pi0

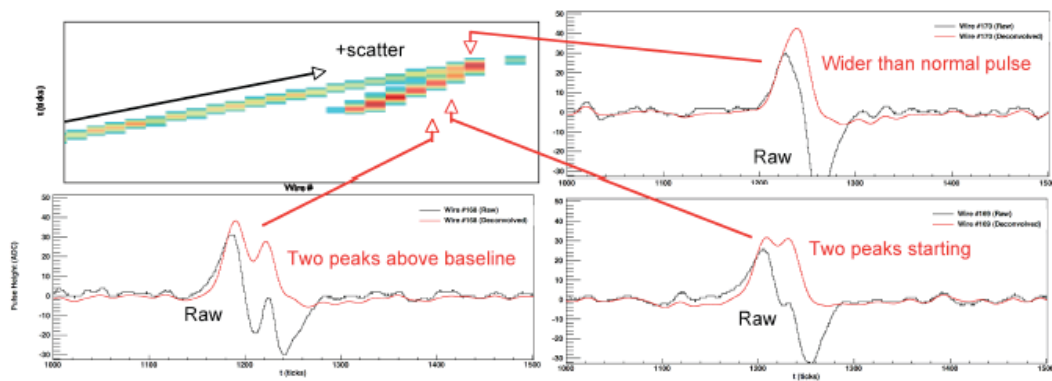


Figure 3: (Upper left) A set of tracks as seen on the (deconvoluted) induction plane. The wire views on three adjacent wires are also shown in order to demonstrate the effects of deconvolution on the raw wire pulses. The raw data can be seen in black and the deconvoluted data can be seen in red.

Figure 1.15: Figure from the ArgoNeuT draft NIM paper.

Argo-decon

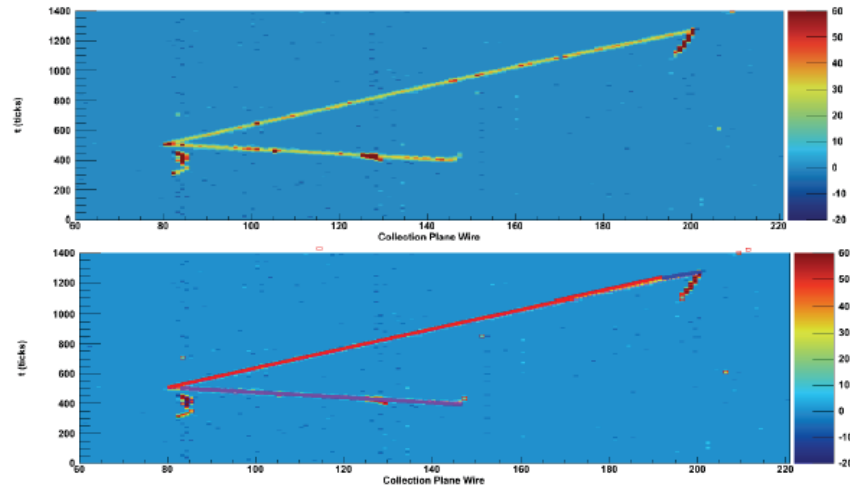


Figure 6: (Top) A neutrino candidate in ArgoNeuT as seen on the collection plane. (Bottom) The Hough lines found with the line-finding algorithm overlaid on the particle tracks.

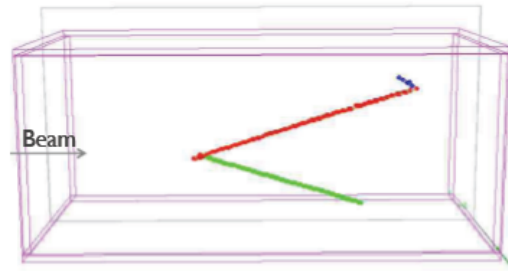


Figure 7: The neutrino event shown in Figure 6 reconstructed in three dimensions.

Figure 1.16: Figure from the ArgoNeuT draft NIM paper showing the status of 3D reconstruction

ArgoNeuT_3Drec

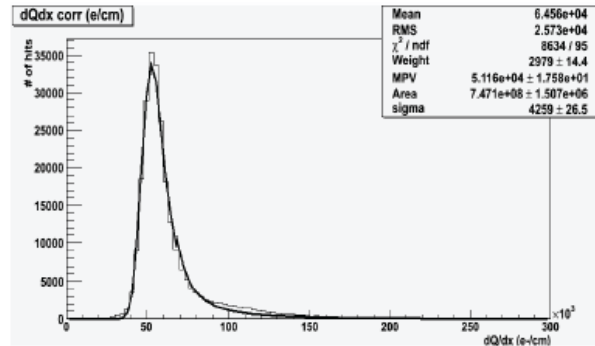


Figure 13: dQ_0/dx distribution (in ADC/cm) obtained for the through-going muon data sample having corrected for the electron lifetime and quenching effect on the ionization charge and properly taken into account the contribution due to δ -rays, as reported in the previous Section. A Landau-Gaussian fit is also reported.

Figure 1.17: Figure from the ArgoNeuT draft NIM paper showing the status of calorimetric reconstruction.

ArgoNeuT-calor

1 understanding of neutrino interactions in LAr. Because MicroBooNE is at the sur-
 2 face, it will also have a large sample of cosmic rays with which it can study potential
 3 backgrounds to rare physics. The process of designing MicroBooNE has naturally
 4 stimulated several developments helpful to the LBNE program. Studies of wire ma-
 5 terial, comparing Be-Cu with gold-plated stainless steel in terms of their electrical
 6 and mechanical properties at room and LAr temperatures, and techniques for wire-
 7 tension measurement are immediately relevant. Expertise has been developed gen-
 8 erating simulations of electrostatic-drift fields as well as simulations of temperature
 9 and flow distributions in LAr cryostats which is being applied to the LAr-FD TPC
 10 and cryostat. MicroBooNE will use the front end of the proposed in-liquid electronics
 11 as the wire-signal amplifiers and the DAQ developed for MicroBooNE will exploit
 12 compression and data-reduction techniques to record data with 100% livetime.

13 In summary, MicroBooNE's LArTPC development goals that are pertinent to LAr-
 14 FD are

- 15 • large-scale testing of LBNE cryogenic front-end electronics, similar in scale to
- 16 the CERN prototype
- 17 • testing of continuous data-acquisition algorithms
- 18 • refinement of the analysis tools developed in ArgoNeuT
- 19 • provide costing and construction lessons-learned

1.4 Summary

Impressive progress has been made in the development of LArTPC technology over the last few years. All elements of the development program have completed the R&D phase. Credible conceptual designs exist for all systems in LAr-FD. The technical activities described in this chapter are properly characterized as preliminary engineering design.

The most significant deficiency is the lack of fully-automated event reconstruction. Algorithms have been developed within the LAr community and are being successfully applied to ArgoNeuT data as well as to simulated MicroBooNE data. The algorithms have individually shown that the high efficiency and excellent background rejection capabilities of an LArTPC are achievable. The task remains to combine them into a single package.